Contents lists available at ScienceDirect

Comptes Rendus Geoscience

www.sciencedirect.com

Tectonics, tectonophysics

New sedimentological, structural and paleo-thermicity data in the Boucheville Basin (eastern North Pyrenean Zone, France)

Roman Chelalou [a,*], Thierry Nalpas [a], Romain Bousquet [a], Maxime Prevost [c], Abdeltif Lahfid [b], Marc Poujol [a], Jean-Claude Ringenbach [c], Jean-François Ballard [c]

[a] Géosciences Rennes, UMR 6118, Université de Rennes-1–CNRS, Campus de Beaulieu, 35042 Rennes cedex, France
[b] BRGM, 3, avenue Claude-Guillemin, 45100 Orléans, France
[c] TOTAL, CSTJF, avenue Larribau, 64018 Pau cedex, France

A B S T R A C T

The Boucheville Basin is one of the easternmost Mesozoic basins of the North Pyrenean Zone (NPZ) that was opened during the Albian extension between the Iberian and European plates. During the extension, a HT/LP metamorphism event affected the Albian basins near the North Pyrenean Fault (NPF). Our aim is to better understand the evolution of the Boucheville Basin during the Albian–Cenomanian lithospheric thinning, which occurred under high thermal conditions. Sedimentological and structural data were collected in the basin and are used to produce synthetic stratigraphic columns of different portions of the basin and to restore selected cross-sections. North–south cross-sections show that the Boucheville Basin is a large and asymmetrical deformed syncline with inverted borders. Synthetic stratigraphic columns show that the sedimentation of the Boucheville Basin starts with carbonate platforms deposited under low bathymetric conditions showing slope deposits and evolves to deep bathymetric conditions of marls deposited without evidence of slopes. Raman spectroscopy on carbonaceous material (RSCM) was made on samples used to construct the sedimentological stratigraphic columns in order to obtain a temperature map of the Albian metamorphism. They reveal homogeneity in the temperatures between 500 and 600 °C. In situ LA–ICP–MS U–Pb dating of titanite grains found in a syn-deformation located in the Albian calcschists provided an age of ca. 97 Ma that gives a time constraint for both the deformation and metamorphism. These data are used collectively to propose a model for the tectono-sedimentary and metamorphic evolution of the Boucheville Basin during the Albian extension.

1. Introduction

The N110°-trending Pyrenean belt (Fig. 1), separating the Iberian microplate from the European plate, is a narrow 400-km-long continental belt that developed in response to the collision between the Iberian microplate and the European plate during the Late Cretaceous and the Tertiary (Beaumont et al., 2000; Chevrot et al., 2015; Choukroune, 1989; Deramond et al., 1993; Muñoz, 1992; Roure and Choukroune, 1998; Teixell, 1998). Triassic, Jurassic and Cretaceous rifting events preceded the development of the Pyrenean belt that mainly resulted in the inversion of the

Lower Cretaceous basins (Puigdefabregas and Souquet, 1986; Vergés and García-Senz, 2001). The Lower Cretaceous rifting in the Pyrenean area, coeval with the opening of the Bay of Biscay, was related to the anticlockwise rotation of the Iberian microplate relative to the European plate (Choukroune and Mattauer, 1978; Gong et al., 2008; Jammes et al., 2009; Le Pichon et al., 1968; Olivet, 1996; Rosenbaum et al., 2002; Sibuet et al., 2004). These east–west-oriented basins, created during this rifting at the northern border of the future Pyrenees, are well known for their high-temperature metamorphism, which is synchronous with the Aptian–Albian deposits (Albarède and Michard-Vitrac, 1978; Bernus Maury, 1984; Casteras, 1933; Choukroune, 1970; Mattauer, 1968; Montigny et al., 1986; Ravier, 1959; Verschure et al., 1969).

In the North Pyrenean Zone (NPZ), occurrences of subcontinental mantle rocks (peridotites) associated with Mesozoic sedimentary formations (Fig. 1b) were described early by Lacroix (1895), and their origin has been debated for more than 100 years. Recent studies in the NPZ have interpreted some of these lherzolites as subcontinental mantle material reworked through sedimentary processes within Cretaceous basins (Lagabrielle and Bodinier, 2008). They proposed that the exhumation of the subcontinental mantle was associated with continental thinning during the Mid-Cretaceous Pyrenean rifting (Clerc and Lagabrielle, 2014; Clerc et al., 2015; Lagabrielle et al., 2010). That was also proposed for the Mauléon Basin based on the interpretation of the geophysical profiles and fieldwork (Jammes et al., 2009; Masini et al., 2014).

The NPZ is currently considered as a former rift system (Tugend et al., 2014, 2015) that has been affected by HT metamorphism during lithospheric thinning (Fig. 1c) (Clerc and Lagabrielle, 2014; Clerc et al., 2015; Golberg and Leyreloup, 1990). Since the NPZ basins were exhumed during the Pyrenean compression, they are potential analogues for depicting passive margins that recorded a HT metamorphism. These HT margins show original geometry, thermal evolution and subsidence (Clerc and Lagabrielle, 2014; Clerc et al., 2015; Vacherat et al., 2014). The present study aims at assisting in the understanding of the tectono-sedimentary evolution of extensional basins such as the Boucheville Basin under high thermal conditions.

2. Geological setting

The Boucheville Basin is located in the southeastern part of the NPZ, just north of the North Pyrenean Fault (NPF). It extends on 30 km, from the Bessède Massif (to the West) to the Agly Massif (to the East), and is 7 km broad in its widest part (Fig. 1). The NPF separates the NPZ from the Axial Zone (AZ) (Fig. 1). In the southern part of the NPZ, near the NPF, the biostratigraphical record is erased; this is probably due to intense metamorphism. Therefore, in the Boucheville Basin, the ages of the sediments are usually determined through facies analogy with those from the less metamorphic Saint-Paul-de-Fenouillet Basin. This basin is located on the North of the Boucheville Basin on the other side of the Agly Massif (Fig. 1. b). The sediments
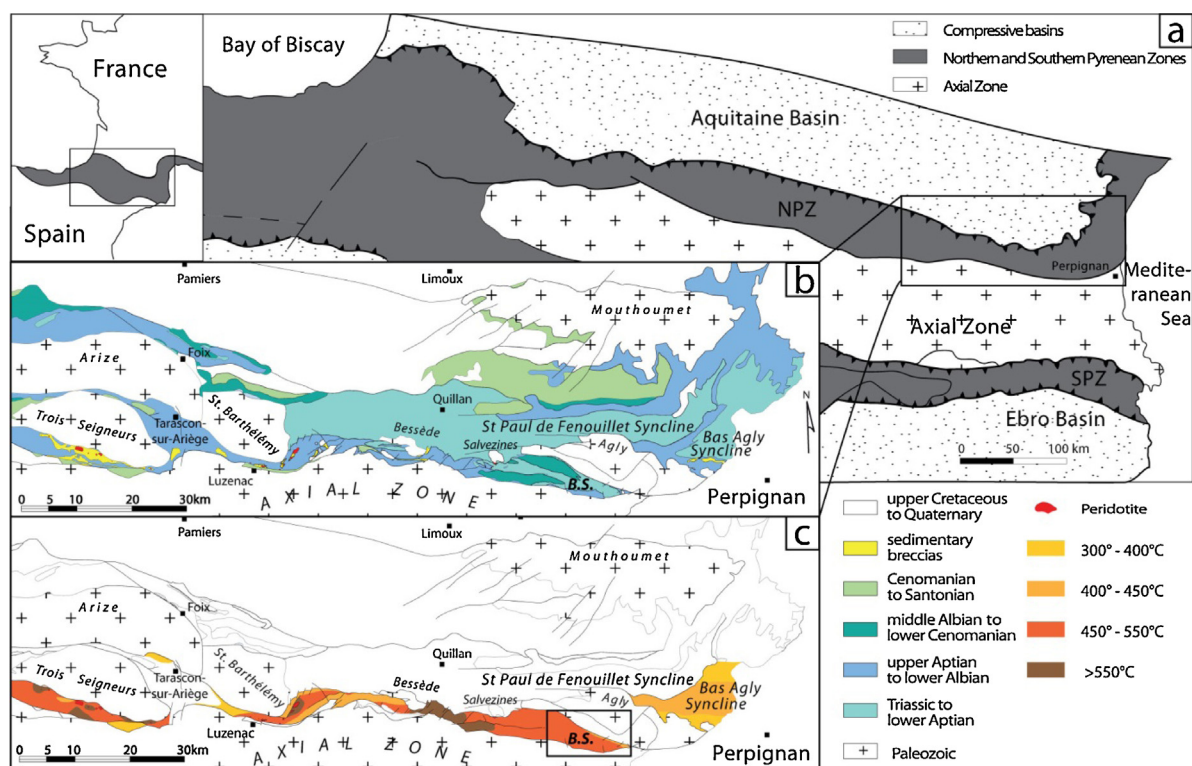

Fig. 1. (a) Structural map of the Pyrenees. (b) Geological map of the Northeastern Pyrenees modified from Clerc (2012). (c) Synthesis of known temperatures in the metamorphic Mesozoic basins of the NPZ (modified from Clerc, 2012). B.S.: Boucheville syncline.
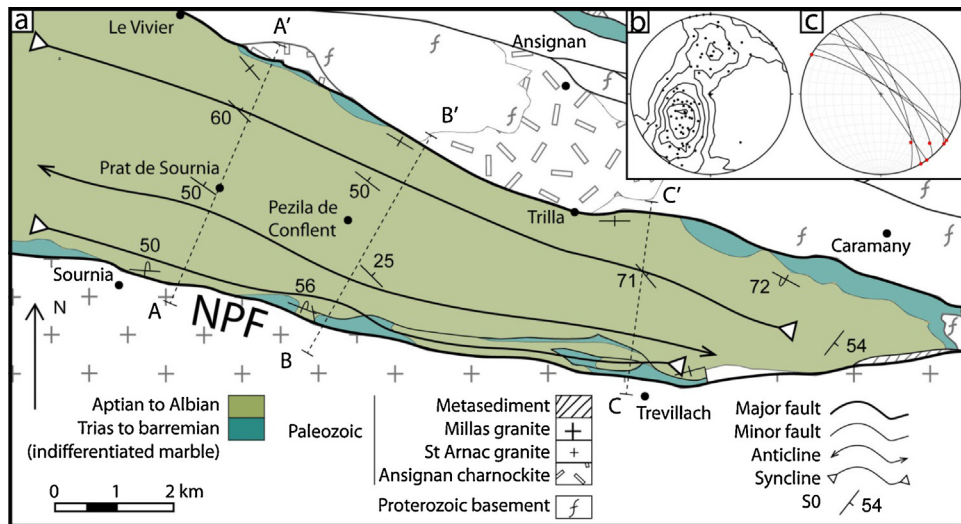
Fig. 2. (a) Structural and geological map of the eastern part of the Boucheville Basin with location of the cross-sections presented in Fig. 6. Modify after Fonteilles et al. (1993). (b) Stereogram of stratification plans poles. (c) Stereogram of isoclinal folds plans and hinges.

of the basin of Saint-Paul-de-Fenouillet are well dated (Berger et al., 1993), especially the Neocomian carbonate platforms and Albian marls, which were dated by ammonites (Collignon et al., 1968). The Saint-Paul-de-Fenouillet Basin is therefore a reference for indirect dating of metamorphosed sedimentary series in the area.

This study focuses on the eastern part of the Boucheville Basin (Figs. 1 and 2a). It was previously described as a synclinorium where three phases of deformation were recognized (Choukroune, 1970). According to Choukroune (1970), by comparison with other tectonic events already documented in the Pyrenees, the first one is a ductile compressional phase associated with high wavelength folds. The second is a ductile compressive dextral phase with short-wavelength folds (both Late Cretaceous). The third is a brittle compressive phase (Eocene).

The sediments of the Boucheville Basin consist of three different lithologies (Bernus Maury, 1984). The first lithology is inhomogeneous marbles which form the basis of the basin. These marbles may contain thin phyllitic beds (rich in alumina), and some retrograde metamorphosed orthoclase and/or scapolite porphyroblasts have been reported (Bernus Maury, 1984). This author also observed interbedded lenses rich in metamorphic minerals (clinopyroxene, green amphibole, feldspars, biotite, and scapolite). The second lithology is a calcschist previously described by Bernus Maury (1984) as sandstone composed of small rounded quartz grains (50 to 100 μm). The rocks are flattened, with a well-defined schistosity outlined by some biotite lamellas and opaque materials. The last lithology is a rock called "hornfels of Vira" by Ravier (1959) who did not notice the preferred orientation shown by the metamorphic assemblages. Even though the "hornfels of Vira" do not properly result from contact metamorphism (see below), we will use that classical terminology hereafter. These rocks are rich in round or almond-shaped plagioclase (80% of the rock) bordered by black mica (Bernus Maury, 1984; Ravier, 1959). The last

two lithologies are stratigraphically located over the marbles, but no particular organization was documented according to these authors.

In the Boucheville Basin, the maximum temperature recorded is $570 \pm 10\,°C$ in the west and decreases to 400-450 °C in the east (Golberg and Leyreloup, 1990) (Fig. 1c). In the nearby Pays de Sault (between the Bessède Massif and the Saint-Barthélémy Massif, Fig. 1), there is a direct relationship between exhumed mantle, the thickness of the crust and the degree of metamorphism. Close to the lherzolites, the degree of metamorphism is the highest and the maximum temperatures estimated are higher than 600 °C (Golberg and Leyreloup, 1990).

3. Results

3.1. Stratigraphy

We present a map of the eastern part of the Boucheville Basin and the cross-sections associated with the stratigraphic columns (Figs. 2 and 3). Fig. 3a represents four stratigraphic columns built from section A–A' that illustrate, from south to north, the four sides of the two synclines (Fig. 2). Based on mapping, field observations and thin sections data, a general synthetic stratigraphic column of the basin allows us to reconstruct a general evolution of the depositional environments (Fig. 3b). Three main lithologies can be defined: marbles, hornfelses and black calcschists.

Marbles form the base of the Mesozoic sedimentary series (Fig. 3b, Sms, e and f). Because of the lack of biomarkers, the marbles from the Boucheville Basin were not directly dated. We cannot conclude whether this lack was primary or due to metamorphic erasing. However, by correlation with similar limestones/marbles from the nearby Saint-Paul-de-Fenouillet Basin, Jurassic and Berriasian (equivalent to the Urgonien facies) ages have been proposed (Berger et al., 1993; Collignon et al., 1968). These
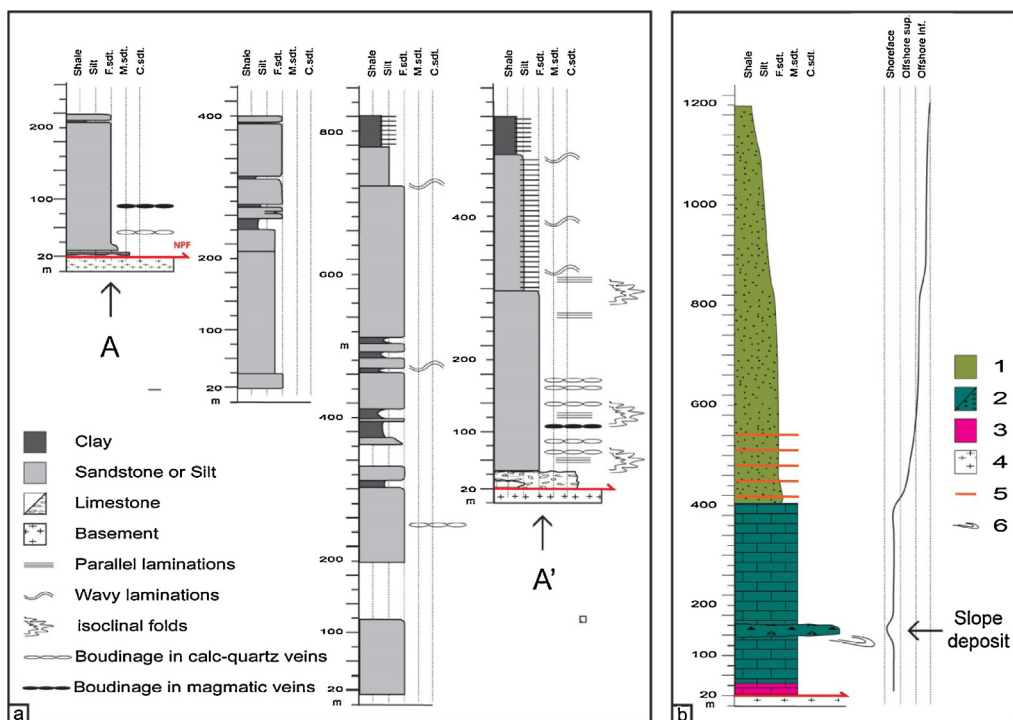
Fig. 3. (a) Four stratigraphic columns made along the section A–A', from south to north, reflecting the thickness variations in the basin and the preferential localization of the deformation along the northern edge. (b) Synthetic stratigraphic column of the basin, the change in the depositional environments illustrates the deepening of the basin. 1, Aptian–Albian; 2, Jurassic to Berriasian; 3, Triassic; 4, basement; 5, carbonate interbedded layers; 6, slump.

marbles are composed of fully recrystallized limestones and of the following metamorphic minerals: scapolite, diopside, K-feldspar, plagioclase, biotite, phlogopite, and pyrite. To the east of the basin, saccharoid white or yellow marbles are outcropping, occasionally associated with cargneules, probably Triassic in age (Berger et al., 1993). These are discontinuous and can reach a maximum thickness of 10 m (Fig. 3b). On the northern and southern borders of the basin, a white marble with grey levels is observed and is associated with the Jurassic and Lower Cretaceous (Berriasian) (Berger et al., 1993). This series of marbles reaches a maximum thickness of 400 m and presents boudinaged morphology in the map (Fig. 2). Furthermore, we observed boudinaged sills at the centimetric scale (see below), and boudinage at the decimetric to plurimetric scale has been documented in the Boucheville Basin marbles (Clerc and Lagabrielle, 2014). The base of these marbles presents stratifications with alternations of slumps and monogenic to polygenic sedimentary breccias (Sm. 1e), some of which contain decimetric clasts from the Proterozoic–Paleozoic basement. Supplementary material 1f presents a cross-section of a slump in marbles showing feldspar clasts. These slumps and breccias are related to slopes located at the basin border. These sedimentary structures are good polarity criteria for structural reconstruction. The top of these marbles presents carbonate platform sedimentation without slumps or breccias.

The contact between the marbles and the black calcschists is gradual over 10 m, without deformation.

The thickness of the calcschists is 200 m in the north and 1000 m in the south (Fig. 3), and is related to the asymmetry of the basin. The change in the depositional environment from the Berriasian to the Albian implies an increase in subsidence and in the deepening of the basin during the Aptian–Albian deposition. As for the marbles, the age of the calcschists is suggested by facies comparison with less metamorphic basins from the northern part of the NPZ (Berger et al., 1993; Collignon et al., 1968). These calcschists are extremely homogeneous, with a quartz grain size varying from very thin (80–70 μm) to silt (Fig. 3, Sms. 1b and d), with angular grains (Sm. 1d). Several layers are devoid of quartz (Sms. 1c and d), and because of the excess of calcite, of the presence of only a few silicate minerals and the lack of quartz sills, we believe that this lack of quartz grains is primary and not due to metamorphism.

In the South of the basin, between Sournia (south) and Vira (north), the base of the calcschist series is made of a formation rich in plagioclase and K-feldspar porphyroblasts (100 to 500 μm in size) embedded in a calcite cement (Sm. 1a). The feldspar grains are surrounded by biotite and opaque filaments, but the rock is devoid of quartz. This formation corresponds to the "hornfels of Vira" from the literature (Bernus Maury, 1984; Ravier, 1959). The macroscopic aspect of this formation is similar to that of the other calcschists, and thus it is impossible to precisely determine its thickness. Nevertheless, using thin sections reported on the stratigraphic column to determine the variations in the lithology, the thickness of the so-called "hornfels" can be estimated at 200 m at its most. The dark color of the whole series indicates the presence of large quantities of organic matter (Sm. 1a). The thickness

and homogeneity of the series prevent us from considering these hornfels as the result of a contact metamorphism. Furthermore, we can estimate that the protolith is substantially different, and is probably composed of marls containing sufficient clay to supply the aluminum required for the formation of plagioclase.

On the northern edge of the basin, where the "hornfels" do not outcrop, the base of the calcschists series presents interbedded carbonate layers with parallel or wavy laminations (Sms. 1c and d), suggesting tidal or storm deposits. However, the transition from platform sedimentation (Lower Mesozoic limestone/marbles) to a lower offshore sedimentation Cretaceous calcschists, Fig. 3) implies deepening, favoring storm deposits. The homogeneity of this series indicates a constant depositional environment located in the lower offshore. The lack of turbidites suggests the absence of significant slopes in the Boucheville Basin during Albian time. The transition from an isopach carbonate platform (marbles) to an asymmetrical deposit of lower offshore sedimentation (calcschists) implies a decrease in the wavelength of the deformation, with the creation of a sub-basin (namely the Boucheville Basin). The lack of slope during the Albian is thus consistent with accommodation related to flexuration at local scale. In all these Mesozoic series, we observe that S1 is parallel to S0, and therefore S1 is useful to find S0 in the homogeneous calcschists when the stratigraphy is not clear.

3.2. Structure and deformation

The map and the cross-sections present two ENE–WSW-trending isoclinal synclines parallel to the basin borders (Figs. 2a and 2b). The southern one is 1 km wide and sometime partially deformed by reverse faults to the south of the basin, while the northern one is about 2 km wide.

The southern border of the basin is the NPF, where the granite of Millas thrusts over the Boucheville Basin to the north. The northern edge of the basin is a vertical or north-dipping reverse fault, which brought in contact the Proterozoic series of the Agly massif and the Boucheville Basin. Reverse borders, reverse faults to the south and the basin general folded structure illustrates the major part of the compressional deformation.

In this section, we will focus on the extensional deformations and relationships with metamorphism.

In all these Mesozoic series, we observe foliation S1, which in most cases is subparallel to stratification S0. This foliation is the axial plane of isoclinal folds (see below) whose axis direction, variable, is parallel to the lineation of intersection S1–S0 (L1) and is very often emphasized by metamorphic minerals (Choukroune, 1970) such as biotite, plagioclase diopside, and scapolite.

The most important and penetrative deformations are observed in a zone that is approximately 500 m wide along the northern border of the basin. This zone is stratigraphically located at the base of the Aptian–Albian calcschists series. Boudinaged calc-quartz veins (Sm. 2a) resulting from Mesozoic metamorphism (Boulvais, 2016), isoclinal folds (Fig. 2c, Sms. e and f) and boudinage

in interbedded carbonate layers are observed. The boudinaged veins are usually subparallel to the stratification, but some are deformed by the isoclinal folds and crosscutting them (Sms. 2e and f). Therefore, we may assume that the isoclinal folds are contemporaneous with the growth of these veins.

Deformation is much more localized and less penetrative on the southern edge of the basin. In the village of Sournia (Fig. 2), the low-dipping S0/S1 is deformed by high-dipping shearing (C, with N20 and N40–trending stretching lineation) producing sigmoidal structures (Sms. 2c and d). Sigmoidal deformation localized along the contact suggests a relatively brittle deformation of the carbonate layers. However, we failed to determine whether these deformations were due only to the Pyrenean compressive phase or to the Albian extensional phase with later reactivation during compression.

Magmatic sills (east of Sournia on the road to Prat de Sournia to the south (Fig. 4 star 4) and close to the Vivier village to the north, Fig. 4, star 3) can be distinguished from the calcite- and quartz-rich veins studied by Boulvais (2016). These sills occur in the "hornfels" series or at the base of the black calcschists. They are plurimetric in length and millimetric to centimetric in thickness and present a strong boudinage (Sm. 2g). The mineralogical composition of these sills is described below.

In the East of the basin at the base of the calcschists series, on the road to Montalba, we notice occurrences of metamorphic diopside. These diopsides recorded at least two strain regimes: a syn-metamorphic one (S1), showing rotations and pressure shadow patterns (Sm. 2b) and a second one, with fold S1 and the stratification (Sm. 2b). However, the whole structure has been affected by the later Pyrenean compression, as indicated by many reverse faults in the South of the basin.

3.3. Metamorphism

The Mesozoic extension caused an extreme lithospheric thinning with mantle exhumation (Clerc, 2012; Clerc and Lagabrielle, 2014; Clerc et al., 2015; Jammes et al., 2009; Lagabrielle and Bodinier, 2008; Lagabrielle et al., 2010; Tugend, 2013; Tugend et al., 2015), and the rise of the mantle
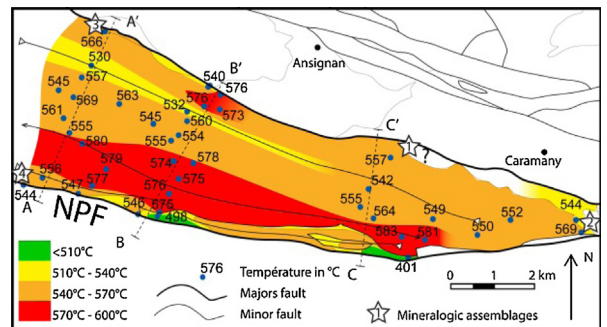

Fig. 4. Map of the maximum temperatures recorded during the Mesozoic metamorphism measured by Raman spectroscopy and the characteristic mineralogical assemblages. Data are detailed in supplementary material #3.

produced a HT/LP metamorphism that is characteristic of the area (Clerc, 2012; Clerc and Lagabrielle, 2014; Clerc et al., 2015; Golberg and Leyreloup, 1990; Ravier, 1959). We sampled the Boucheville Basin to get more data about the temperature evolution at the scale of the basin by producing a temperature map by Raman spectroscopy.

The metamorphic overprint in the basin is indicated by the following mineral assemblages: (1) In the marbles: tremolite, chlorite and phlogopite-rich biotite (Fig. 4, star 1) or pure phlogopite, diopside, plagioclase and K- feldspar (Fig. 4, stars 2, Sms. 2.b and 4.a1); and (2) in the magmatic sills to the east of Sournia (Fig. 4, star 4): quartz, feldspar, chlorite, tremolite, muscovite, biotite, and phlogopite. To the south of Vivier (Fig. 4, star 3 and Sm. 2.g): microcline, titanite, biotite, plagioclase and apatite (see Supplementary material); the titanite grains were used to date the sill (see below). Generally, anorthite-rich plagioclase grains form typical syn-metamorphic porphyroblasts, growing onto some large K-feldspar crystals, probably of detrital origin (disaggregation of the nearby Ansignan charnockite or granite?). Some K-feldspar grains occur as small (millimeter) grains in thin sections and have a metamorphic origin. From the diopside and scapolite occurrences, Golberg and Leyreloup (1990) estimated a metamorphic peak temperature between 400 °C in the western part to 500 °C in the eastern part of the basin. These temperature conditions are slightly lower than our estimate using the RSCM geothermometer.

3.3.1. Raman spectroscopy

The Raman spectroscopy has been used successfully on 43 samples in the Boucheville Basin to characterize the structural evolution of carbonaceous materials (CM), reflecting a transformation from disordered to well-ordered CM during metamorphism (Wopenka and Pasteris, 1993). The irreversible polymerization and reorganization of these materials is reflected in their Raman spectrum by the decreasing width of the graphite G band and the gradual disappearance of the defect bands, first D3 and D4, then D1 and D2. The Raman spectrum of well-ordered CM (perfect graphite) contains only the G band. This spectral evolution with increasing graphitization was related to the temperature and quantified, providing a way to determine the peak temperatures reached by the metamorphic rocks (Beyssac et al., 2002). This is the basis of the Raman spectroscopy CM geothermometer (RSCM), which was calibrated in the range 330–650 °C by Beyssac et al. (2002), extended to the range 200–320 °C (Lahfid et al., 2010) and 100–200 °C (Lahfid et al., 2014). For our concern (Sm. 3), RSCM has been calibrated for the range 200–640 °C with an absolute accuracy of ± 50 °C and a much better internal reproducibility of about 10–15 °C (Lahfid et al., 2014). This approach, associated with petrological observations, may allow us to distinguish the different thermal and structural events (Wiederkehr et al., 2009; Wiederkehr et al., 2011).

As a first-order result, high-temperature homogeneity bracketing between 530 and 580 °C is observed, except for a few areas separated by tectonic structures (Fig. 4). This temperature uniformity is consistent with the existence of an overlaying sedimentary cover, the thickness of which will be discussed later.

3.3.2. P–T estimations

In addition, to better constrain the metamorphic evolution of the sediment outcropping in the basin, we performed P–T estimations using a thermodynamic approach for one sample (sample B01363, Fig. 4, star 2 and Sm. 2.b). All calculations were performed by minimizing Gibbs-free energy (De Capitani and Brown, 1987) using the software suite Theriak-Domino (De Capitani and Petrakakis, 2010) and the JUN92d.bs database.

The studied sample is a marble containing diopside about 1 mm wide and 5 mm long. The metamorphic mineralogical assemblage documenting the temperature peak reached by the sample (Fig. 6, star 2 and Sm. 2.b) is made of diopside-rich clinopyroxene–anorthite–phlogopite-rich biotite–orthoclase (K-feldspar)–calcite–pyrite (Sm. 4.a1). Rare small quartz grains have been identified using the microprobe. They are always occurring between diopside and anorthite crystals (Sm. 4.a2). In our opinion, this texture indicated a clear growing of quartz after the diopside. These quartz grains are clearly postdating the temperature peak. We note also the occurrence of some large K-feldspar clasts of detrital origin. For the modelling, to account for the occurrence of pyrite in the rock, we use a magnetite (Mt) as an O_2 buffer. The stability field of the studied mineralogical assemblage is large, with a T-range of at least 200 °C, and does not provide any good constraints for the pressure. This assemblage can be stable up to 0.8 GPa (Sm. 4.b). In $T-X_{CO_2 H_2 O}$ diagrams, the stability field of the T-peak assemblage is strongly P-dependent (Sm. 4.c) and it is constrained by the quartz-appearance reaction. By decreasing the pressure by 0.15 GPa, the peak temperature may decrease by 60 °C. During a progressive isobaric heating of carbonate-rich rocks as siliceous dolomites, the fluid composition will change: the occurrence of diopside in such rocks is only possible if CO_2 activity increases until reaching a value around 0.8 (Brown and Skinner, 1974; Bucher and Frey, 1994). Higher values of X_{CO_2} will decrease the stability field of H_2O-bearing mineral, as biotite. Knowing the peak temperature reached by this sample (580 °C) by Raman thermometry, we compute the $P-X_{CO_2 H_2 O}$ diagram to know the maximum sedimentary thickness of the basin. Considering a X_{CO_2} around 0.8, the pressure cannot exceed 0.35 GPa. At higher pressures, assemblages containing quartz will be stable (Sm. 4.b). However, the observed mineralogical assemblage in sample BO1363 will be still stable at pressures lower than 0.35 GPa. As a second-order result, we observe that the isotherms are roughly parallel to the stratigraphic bedding and appear to follow the basin's double syncline structure. On the map of Fig. 4, the highest temperatures are observed in the core of the folded structure and are associated with the deepest levels of the basin. Based on these stratigraphic-thermal correlations, we estimate the minimum temperature gradient in the basin to be between 70 °C/km and 80 °C/km.

3.3.3. U–Pb geochronology

In order to obtain a geochronological constraint on the metamorphism and the deformation, we performed in situ LA–ICP–MS U–Pb dating of the titanite grains found in the

magmatic sill described previously (Sm. 2.g). Dating was performed directly in thin sections at Géosciences Rennes using an ESI NWR193UC Excimer laser coupled with an Agilent 7700 × quadripole ICP–MS. The analytical procedure is detailed in Boutin et al. (2015). Five titanite grains (Sm. 6.a) were analyzed (24 analyses) and the data can be found in the Supplementary material. Plotted in a Tera–Wasserburg diagram (Sm. 6.b), the data define a discordia with a lower intercept date of 97 ± 2.3 Ma (MSWD = 3.9). If the discordia is anchored to the common Pb value calculated following the model of Stacey and Kramers (1975), we end up with a lower intercept date of 99 ± 1.5 Ma equivalent within the margin of error. Therefore, we interpret this date of ca 97 Ma as the crystallization age of these titanite grains.

4. Interpretation and discussion

Thickness variations and lateral facies variations between the edges and the center of the basin allow us to suggest that the Boucheville Basin was an independent basin or a subbasin separated from the Saint-Paul-de-Fenouillet Basin by the shoal, which was the Agly Massif during the Cretaceous extension. Based on geological maps, isotherms map and inferred cross-sections, we suggest that the current architecture of the basin corresponds to a large syncline having two reversed flanks with opposite verging. Choukroune (1970) described the "synclinorium" structure of the Boucheville Basin as the result of the study of foliations, schistosities, and microstructures, with the idea that folds could be formed only in a compressive context. However, our study shows that the isoclinal folds were formed during the Cretaceous extension.

A remarkable feature is the rapid variation in the structure of the Mesozoic marbles interpreted as boudinage. It can be related to a ductile stretching and frequent pinched structure. An asymmetry of the thickness of the calcschists is observed, with a greater thickness of the whole sedimentary pile to the north (Fig. 5).

Penetrative and ductile syn-metamorphic deformation is well developed in a 500-m-wide area on the northern edge of the basin (Fig. 5). In this area, the isoclinal folding and the formation of calcite and quartz-rich veins, which are the direct result of metamorphism (Boulvais, 2016), are coeval. In addition, we dated a boudinaged sill at 97 Ma, which intrudes the calcschists. This sill emplacement is posterior to the deposition of the sediments but anterior and/or contemporary with both metamorphism and deformation (isoclinal folding and boudinage).

Based on the relation between deformation and metamorphism, we suggest that the thermal overprint of the whole basin is contemporaneous with the ductile deformation, and was probably produced by an extreme crustal thinning during the Albian–Cenomanian rifting (Clerc and Lagabrielle, 2014; Clerc et al., 2015; Lagabrielle and Bodinier, 2008; Lagabrielle et al., 2010; Tugend et al., 2014; Vacherat et al., 2014; Vielzeuf and Kornprobst, 1984).

On the southern edge of the basin, the deformation shows brittle features and is more localized along the contact than the one observed on the northern edge of the
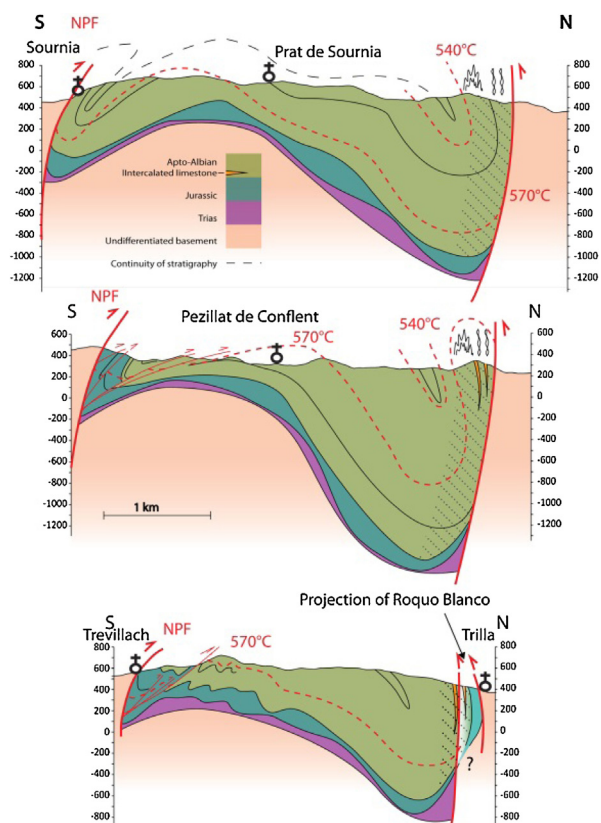

Fig. 5. Cross-section A–A', B–B', and C–C' in the Boucheville Basin with isotherms placed according to the temperature map shown in Fig. 6. The black crosses symbolize the churches in the villages.

basin. This deformation is documented by a well-developed N20/N40 stretching lineation. If we consider the structures observed in the marbles (Sm. 2.c), we cannot exclude that the Pyrenean shortening was responsible for the observed structural features with a complete erasing of previous extensional effects. In addition, the observed shearing indicates a compressional deformation with the bedding now in a reverse position, but may indicate also an extensional deformation if the bedding is restored as being in a normal position.

Deformations and sediment thickness are greater in the north, suggesting more subsidence there. A strong asymmetry for the Boucheville Basin is clearly indicated by the asymmetry of the different structures (Fig. 5) as sediment thickness or intensity and type of deformations. Altogether, we may assume that the main limit, i.e. the area that recorded the highest extension in the Boucheville Basin, is located along its northern border zone.

The minimum temperature gradient (70 °C/km) estimated for the Boucheville Basin is similar to that proposed in other metamorphic Mesozoic basins along the NPZ (Clerc et al., 2015; Vacherat et al., 2014). According to our calculation, pressure was lower than 0.35 GPa. If we assume a pressure value between 0.3 and 0.2 GPa for the temperature peak and a sediment density varying from 2500 to 3000 kg/m³, we estimate the thickness of the

sedimentary cover during the maximum pick of temperature (Albian–Cenomanian) to be between 6 and 10 km

However, regional geological data (geological map of Rivesaltes and Saint-Paul-de-Fenouillet, in prep.) suggest that the sedimentary pile could not have reached such thickness; to the north of Salvezine (Fig. 1), Cenomanian deposits seal the Albian sedimentary pile, which are not exceeding three kilometers in thickness (geological map of Saint-Paul-de-Fenouillet, in prep.). Considering all this, we estimate the thickness of the sedimentary pile during the Albian–Cenomanian metamorphism to be between 6 and 7 km. Therefore, a stronger gradient is needed to explain our measured temperatures and a relative thin sediment cover. Despite slight mappable temperature variations, correlated with the stratigraphy of the basin, we point relative temperature homogeneity between 530 and 580 °C involving a low thermal gradient (see above). This makes the studied case comparable to the Salton Sea basin system, where a very high thermal gradient ($\approx$300 °C/km) is found in the first kilometer of shale sediment, and an almost adiabatic thermal gradient prevailing in the underlying sandstone (Helgeson, 1968).

Mostly focused on the northern edge of the Boucheville Basin, the history of its depositional environments may be outlined as follows.

After an evaporitic event during the beginning of the Triassic, carbonate platforms were deposited from the Liassic to the Berriasian (Fig. 6). The occurrence of slope breccia and slumps in the Mesozoic carbonates announce a change in the basin's topography, probably related to the local exhumation of the basement, which is probably related to deformation and faults creation during rifting initiation (Fig. 6). From Albian times, the basin deepens and sedimentation changes from carbonate platforms to storm deposits followed by lower offshore marls (Fig. 6). The deposits are asymmetrical, but slope deposits are no longer observed. During the increase in temperature, the deformation tends to be localized in the northern edge of the basin, suggesting the formation of a shear zone (roughly 500 m thick, Fig. 6). This shearing seems to be synchronous with the boudinage of the whole basal carbonate series. Altogether, this indicates that the tectonic setting evolves from cold and brittle to hot and ductile during the onset of Boucheville Basin opening.

It is worth noting that the observed thickness variations and the characteristics of the thermal regime during deformation suggest that a boudinage at a crustal scale controlled the shape of the basin. By unfolding its present geometry, we infer that the width of the Boucheville Basin probably did not exceed ten kilometers at the end of the Albian. This model is coherent with the current model, which proposes that the Mesozoic extension caused an extreme lithospheric thinning with mantle exhumation (Clerc, 2012; Clerc and Lagabrielle, 2014; Clerc et al., 2015; Jammes et al., 2009; Lagabrielle and Bodinier, 2008; Lagabrielle et al., 2010; Tugend, 2013; Tugend et al., 2015) and a rise of the mantle which produced the well-known HT/LP metamorphism. We stress the fact that the most significant limitation to the development of a more sophisticated model for the basin evolution is precluded by the lack of biomarkers or of any other way of dating
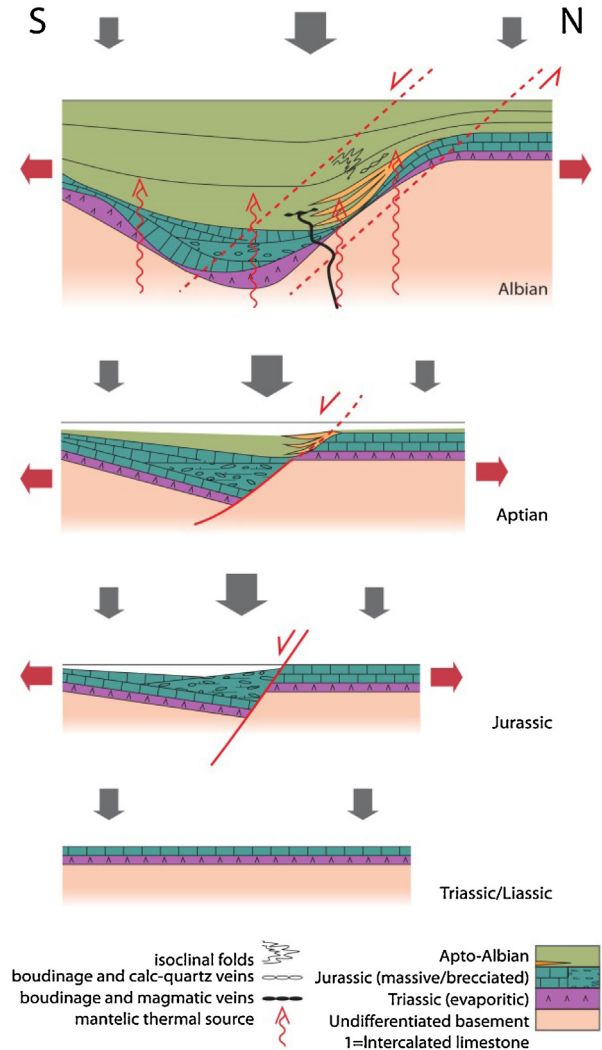

Fig. 6. Tectonic and sedimentological evolution model of the Boucheville Basin, focused on the northern edge of the basin.

deposits. Metamorphism deeply transformed the series and it is therefore risky to compare this basin with the neighboring ones. The presence of a foliation parallel to the bedding complicates the reading of the stratigraphy in a very homogeneous sedimentary sequence such as that of the calcschists of the Boucheville Basin.

5. Conclusion

Our study allowed us to propose a thermal-tectono-sedimentary evolution model, which shows that:

- the Boucheville Basin is a large asymmetric syncline uplifted in its middle part with reverse borders related to the Pyrenean compression. The basin was already asymmetrical when the sediments deposited;
- the Boucheville Basin evolved in two phases: (i) initialization of the rifting in the Jurassic with creation

of the topography, exhumation of the basement and setting up of the slope deposit; the basin subsidence and asymmetry increased during the Cretaceous, and we noticed that more significant boudinage and ductile deformation appear in the northern border;

- the sedimentary evolution, geometry and deformation in the Boucheville Basin allow us to propose that the northern border acted as a main extensional Albian shear zone;

- Raman measurements on organic matter were taken in cohesion with the stratigraphic columns and show that the isotherms are organized subparallel to the basin bedding. These measurements show homogeneous temperatures between 530 and 580 °C, which are coherent with the metamorphic mineral assemblages observed in different parts of the basin;

- the occurrence of magmatic sills at 97 Ma implies the existence of partial melting of the crustal rocks below, related to the crustal thinning and mantle exhumation currently used to explain the HT/LP Pyrenean metamorphism.

Acknowledgments

Appendix A. Supplementary data

Supplementary data associated with this article can be found, in the online version, at http://dx.doi.org/10.1016/j.crte.2015.11.008.

References

Albarède, F., Michard-Vitrac, A., 1978. Age and significance of the North Pyrenean metamorphism. Earth Planet. Sci. Lett. 40 (3), 327–332.

Beaumont, C., Muñoz, J.A., Hamilton, J., Fullsack, P., 2000. Factors controlling the Alpine evolution of the central Pyrenees inferred from a comparison of observations and geodynamical models. J. Geophys. Res. Solid Earth 105 (B4), 8121–8145.

Berger, G., Fonteilles, M., Leblanc, D., Clauzon, G., Marchal, J., Vautrelle, C., 1993. Notice explicative, Carte géologique de la France à 1/50 000, feuille Rivesaltes (1090). Éd. BRGM, Orléans, France, 119 p.

Bernus Maury, C., 1984. Étude des paragenèses caractéristiques du métamorphisme mésozoïque dans la partie orientale des Pyrénées. PhD thesis, Univ. Paris 6, Paris, France, 277 p.

Beyssac, O., Goffé, B., Chopin, C., Rouzaud, J., 2002. Raman spectra of carbonaceous material in metasediments: a new geothermometer. J. Metamorphic Geol. 20 (9), 859–871.

Boulvais, P., 2016. Fluid generation in the Boucheville Basin as a consequence of the North Pyrenean Metamorphism. C. R. Geoscience 348, (this issue).

Boutin, A., de Saint Blanquat, M., Poujol, M., Boulvais, P., de Parseval, P., Rouleau, C., Robert, J.F., 2015. Succession of Permian and Mesozoic metasomatic events in the eastern Pyrenees with emphasis on the Trimouns talc-chlorite deposit. Int. J. Earth Sci. 1–24.

Brown, T.H., Skinner, B.J., 1974. Theoretical prediction of equilibrium phase assemblages in multicomponent systems. Am. J. Sci. 274 (9), 961–986.

Bucher, K., Frey, M., 1994. Petrogenesis of metamorphic rocks. Springer, Berlin, 318 p.

Casteras, M., 1933. Recherches sur la structure du versant nord des Pyrénées centrales et orientales. Bull. Service Carte geol. Fr. 37 (189) 525 p.

Chevrot, S., Sylvander, M., Diaz, J., Ruiz, M., Paul, A., 2015. The Pyrenean architecture as revealed by teleseismic P-to-S converted waves recorded along two dense transects. Geophys. J. Int. 200 (2), 1096–1107.

Choukroune, P., 1970. Contribution à l'étude structurale de la zone métamorphique nord-pyrénéenne ; tectonique et métamorphisme des formations secondaires de la forêt de Boucheville (P.-O.) ; feuille au 1/50 000 Saint-Paul-de-Fenouillet. Bull. BRGM sect 1 (4), 49–63.

Choukroune, P., 1989. The ECORS Pyrenean deep seismic profile reflection data and the overall structure of an orogenic belt. Tectonics 8 (1), 23–39.

Choukroune, P., Mattauer, M., 1978. Tectonique des plaques et Pyrénées ; sur le fonctionnement de la faille transformante nord-pyrénéenne ; comparaisons avec des modèles actuels. Bull. Soc. geol. France 5, 689–700.

Clerc, C., 2012. Évolution du domaine nord-pyrénéen au Crétacé : amincissement crustal extrême et thermicité élevée : un analogue pour les marges passives. PhD thesis, Univ. Paris 6, Paris, France, 249 p.

Clerc, C., Lagabrielle, Y., 2014. Thermal control on the modes of crustal thinning leading to mantle exhumation: Insights from the Cretaceous Pyrenean hot paleomargins. Tectonics 33 (7), 1340–1359.

Clerc, C., Lahfid, A., Monié, P., Lagabrielle, Y., Chopin, C., Poujol, M., Boulvais, P., Ringenbach, J., Masini, E., de Saint Blanquat, M., 2015. High-temperature metamorphism during extreme thinning of the continental crust: a reappraisal of the North Pyrenean paleo-passive margin. Solid Earth Discussions 7 (1), 797–857.

Collignon, M., Fournie, D., Gauthier, J., Lestang, J.D., 1968. Nouvelles données stratigraphiques et sédimentologiques sur le Crétacé inférieur du synclinal de Saint-Paul-de-Fenouillet (Pyrénées-orientales, France). Bull. Centres Recherche de Pau 2 (2), 321–346.

De Capitani, C., Brown, T.H., 1987. The computation of chemical equilibrium in complex systems containing non-ideal solutions. Geochim. Cosmochim. Acta 51 (10), 2639–2652.

De Capitani, C., Petrakakis, K., 2010. The computation of equilibrium assemblage diagrams with Theriak/Domino software. Am. Mineral. 95 (7), 1006–1016.

Deramond, J., Souquet, P., Fondecave-Wallez, M.-J., Specht, M., 1993. Relationships between thrust tectonics and sequence stratigraphy surfaces in foredeeps: model and examples from the Pyrenees (Cretaceous-Eocene, France, Spain). Geol. Soc, London, Spec. Publ 71 (1), 193–219.

Fonteilles, M., Leblanc, D., Clauzon, G., Vaudin, J., Berger, G., 1993. Carte géologique de la France à 1:50000, feuille Rivesaltes (1090). BRGM, Orléans, France.

Golberg, J., Leyreloup, A., 1990. High temperature-low pressure Cretaceous metamorphism related to crustal thinning (eastern North Pyrenean Zone, France). Contrib. Mineral. Petrol. 104 (2), 194–207.

Gong, Z., Langereis, C., Mullender, T., 2008. The rotation of Iberia during the Aptian and the opening of the Bay of Biscay. Earth Planet. Sci. Lett. 273 (1), 80–93.

Helgeson, H.C., 1968. Geologic and thermodynamic characteristics of the Salton Sea geothermal system. Am. J. Sci. 266 (3), 129–166.

Jammes, S., Manatschal, G., Lavier, L., Masini, E., 2009. Tectonosedimentary evolution related to extreme crustal thinning ahead of a propagating ocean: example of the western Pyrenees. Tectonics 28 (4) .

Lacroix, A., 1895. Les phénomènes de contact de la lherzolite et de quelques ophites des Pyrénées. Bull. Carte geol. France 6 (42), 307–446.

Lagabrielle, Y., Bodinier, J.L., 2008. Submarine reworking of exhumed subcontinental mantle rocks: field evidence from the Lherz peridotites, French Pyrenees. Terra Nova 20 (1), 11–21.

Lagabrielle, Y., Labaume, P., de Saint Blanquat, M., 2010. Mantle exhumation, crustal denudation, and gravity tectonics during Cretaceous rifting in the Pyrenean realm (SW Europe): Insights from the geological setting of the lherzolite bodies. Tectonics 29, 4.

Lahfid, A., Beyssac, O., Deville, E., Negro, F., Chopin, C., Goffé, B., 2010. Evolution of the Raman spectrum of carbonaceous material in low-grade metasediments of the Glarus Alps (Switzerland). Terra Nova 22 (5), 354–360.

Lahfid, A., Delchini, S., Brice, L., Hoareau, G., Bourrat, X., 2014. In: Évaluation du degré de maturité de la matière organique par spectroscopie Raman : extension du géothermomètre RSCM vers la gamme 100–200 °C, 24e Réunion des Sciences de la Terre : RST 2014.

Le Pichon, X., Bonnin, J., Pautot, G., 1968. Sea-floor spreading and conti-nental drift. J. Geophys. Res. 73 (12), 3661–3697.

Masini, E., Manatschal, G., Tugend, J., Mohn, G., Flament, J.-M., 2014. The tectono-sedimentary evolution of a hyper-extended rift basin: the example of the Arzacq–Mauléon rift system (western Pyrenees, SW France). Int. J. Earth Sci. 103 (6), 1569–1596.

Mattauer, M., 1968. Les traits structuraux essentiels de la chaîne Pyré-néenne. Rev. Geol. Dyn. Geogr. Phys. 10, 3–11.

Montigny, R., Azambre, B., Rossy, M., Thuizat, R., 1986. K-Ar study of Cretaceous magmatism and metamorphism in the pyrenees: Age and length of rotation of the Iberian Peninsula. Tectonophysics 129 (1), 257–273.

Muñoz, J.A., 1992. Evolution of a continental collision belt: ECORS-Pyre-nees crustal balanced cross-section. In: Mc Clay, K.R. (Ed.), Thrust tectonics. Chapman and Hall, London, pp. 235–246.

Olivet, J., 1996. La cinématique de la plaque ibérique. Bull. Centres Rech. Explor. Prod. Elf Aquitaine 20 (1), 131–195.

Puigdefabregas, C., Souquet, P., 1986. Tecto-sedimentary cycles and de-positional sequences of the Mesozoic and Tertiary from the Pyrenees. Tectonophysics 129 (1), 173–203.

Ravier, J., 1959. Le métamorphisme des terrains secondaires des Pyrénées, Société géologique de France. Mem. Soc. geol. France 38. PhD thesis, Paris, 250 p.

Rosenbaum, G., Lister, G.S., Duboz, C., 2002. Relative motions of Africa, Iberia and Europe during Alpine orogeny. Tectonophysics 359 (1), 117–129.

Roure, F., Choukroune, P., 1998. Contribution of the Ecors seismic data to the Pyrenean geology: Crustal architecture and geodynamic evolution of the Pyrenees. Mem. Soc. geol. France 173, 37–52.

Sibuet, J.C., Srivastava, S.P., Spakman, W., 2004. Pyrenean orogeny and plate kinematics. J. Geophys. Res.: Solid Earth 109, B8.

Stacey, J.T., Kramers, J., 1975. Approximation of terrestrial lead isotope evolution by a two-stage model. Earth Planet. Sci. Lett. 26 (2), 207–221.

Teixell, A., 1998. Crustal structure and orogenic material budget in the west central Pyrenees. Tectonics 17 (3), 395–406.

Tugend, J., 2013. Role of hyperextension for the formation of rift systems and its implication for reactivation processes and orogen formation: the example of the Bay of Biscay and Pyrenees. PhD thesis, Univ. Strasbourg, UDS Strasbourg, France, 288 p.

Tugend, J., Manatschal, G., Kusznir, N., Masini, E., Mohn, G., Thinon, I., 2014. Formation and deformation of hyperextended rift systems: Insights from rift domain mapping in the Bay of Biscay-Pyrenees. Tectonics 33 (7), 1239–1276.

Tugend, J., Manatschal, G., Kusznir, N., 2015. Spatial and temporal evo-lution of hyperextended rift systems: Implication for the nature, kinematics, and timing of the Iberian-European plate boundary. Geology 43 (1), 15–18.

Vacherat, A., Mouthereau, F., Pik, R., Bernet, M., Gautheron, C., Masini, E., Le Pourhiet, L., Tibari, B., Lahfid, A., 2014. Thermal imprint of rift-related processes in orogens as recorded in the Pyrenees. Earth Planet. Sci. Lett. 408, 296–306.

Vergés, J., García-Senz, J., 2001. Mesozoic evolution and Cainozoic inver-sion of the Pyrenean rift. Mem. Mus. natl hist. nat. 186, 187–212.

Verschure, R.H., Hebeda, E.H., Boelrijk, N.A.I.M., Priem, H.N.A., Ave Lalle-mant, H.G., 1969. K-Ar age of hornblende from a hornblendite vein in the Alpine-type ultramafic mass of the Etang de Lers (Ariege), French Pyrenees. Leidse Geologische Mededelingen 42, 59-59.

Vielzeuf, D., Kornprobst, J., 1984. Crustal splitting and the emplacement of Pyrenean lherzolites and granulites. Earth Planet. Sci. Lett. 67 (1), 87–96.

Wiederkehr, M., Sudo, M., Bousquet, R., Berger, A., Schmid, S.M., 2009. Alpine orogenic evolution from subduction to collisional thermal overprint: the $^{40}Ar/^{39}Ar$ age constraints from the Valaisan Ocean, central Alps. Tectonics 28, 6.

Wiederkehr, M., Bousquet, R., Ziemann, M.A., Berger, A., Schmid, S.M., 2011. 3-D assessment of peak-metamorphic conditions by Raman spectroscopy of carbonaceous material: an example from the margin of the Lepontine dome (Swiss central Alps). Int. J. Earth Sci. 100 (5), 1029–1063.

Wopenka, B., Pasteris, J.D., 1993. Structural characterization of kerogens to granulite-facies graphite: applicability of Raman microprobe spec-troscopy. Am. Mineral. 78 (5–6), 533–557.